Exhibit 5

Am J Physiol Heart Circ Physiol
280: H1970–H1981, 2001.

Role of p38 mitogen-activated protein kinase in cardiac myocyte secretion of the inflammatory cytokine TNF-α

CHERRY BALLARD-CROFT, D. JEAN WHITE, DAVID L. MAASS, DIXIE PETERS HYBKI, AND JURETA W. HORTON
Department of Surgery, University of Texas Southwestern Medical Center, Dallas, Texas 75390-9160

Received 25 September 2000; accepted in final form 14 December 2000

Ballard-Croft, Cherry, D. Jean White, David L. Maass, Dixie Peters Hybki, and Jureta W. Horton. Role of p38 mitogen-activated protein kinase in cardiac myocyte secretion of the inflammatory cytokine TNF-α. *Am J Physiol Heart Circ Physiol* 280: H1970–H1981, 2001.—This study examined the hypothesis that burn trauma promotes cardiac myocyte secretion of inflammatory cytokines such as tumor necrosis factor (TNF)-α and produces cardiac contractile dysfunction via the p38 mitogen-activated protein kinase (MAPK) pathway. Sprague-Dawley rats were divided into four groups: *1*) sham burn rats given anesthesia alone, *2*) sham burn rats given the p38 MAPK inhibitor SB203580 (6 mg/kg po, 15 min; 6- and 22-h postburn), *3*) rats given third-degree burns over 40% total body surface area and treated with vehicle (1 ml of saline) plus lactated Ringer solution for resuscitation (4 ml·kg^{-1}·percent burn^{-1}), and *4*) burn rats given injury and fluid resuscitation plus SB203580. Rats from each group were killed at several times postburn to examine p38 MAPK activity (by Western blot analysis or in vitro kinase assay); myocardial function and myocyte secretion of TNF-α were examined at 24-h postburn. These studies showed significant activation of p38 MAPK at 1-, 2-, and 4-h postburn compared with time-matched shams. Burn trauma impaired cardiac mechanical performance and promoted myocyte secretion of TNF-α. SB203580 inhibited p38 MAPK activity, reduced myocyte secretion of TNF-α, and prevented burn-mediated cardiac deficits. These data suggest p38 MAPK activation is one aspect of the signaling cascade that culminates in postburn secretion of TNF-α and contributes to postburn cardiac dysfunction.

rat model of burn trauma; Langendorff perfusion; cardiac contraction-relaxation; tumor necrosis factor-α

IN SEVERAL INJURY AND DISEASE STATES inflammatory cytokines such as tumor necrosis factor (TNF)-α play a significant role in the inflammatory sequelae that culminates in multiple organ failure. Recent studies (7–10, 25, 33, 39, 44, 48, 58) have shown that cardiac myocytes themselves secrete inflammatory cytokines in response to trauma or sepsis, producing myocardial cytokine levels that exceed those measured in the systemic circulation. In addition, cardiac secretion of the inflammatory cytokine TNF-α has been shown to correlate with cardiac contraction and relaxation deficits (7, 25) and has been proposed to mediate cardiac deficits in burn trauma (32, 34), ischemia-reperfusion (44), and hemorrhagic shock (45). Anticytokine strategies such as monoclonal antibodies to TNF-α have had limited success in models of ischemia-reperfusion, trauma, or sepsis (1, 2, 19–21). Recent approaches to limiting cytokine-mediated organ injury and dysfunction have included defining the signal transduction pathways that regulate cytokine synthesis, with the goal of developing therapeutic approaches to interrupt specific aspects of this pathway (10). This approach could limit cardiodepression mediated by cardiac cytokine secretion without producing generalized immunosuppression or increasing susceptibility to subsequent infection.

One aspect of the signal transduction pathway that regulates cytokine synthesis in other cell populations is the p38 mitogen-activated protein kinase (MAPK). Activation of the p38 MAPK signaling cascade is one of the mechanisms by which cells respond to environmental stress (47). In fact, p38 was first identified as a protein undergoing rapid tyrosine phosphorylation after exposure to lipopolysaccharide (LPS), a bacterial surface component released on host infection (28). Later, Lee and colleagues (41) described a protein that was the binding site for pyridinyl imidazole compounds that had been shown to inhibit LPS-stimulated inflammatory cytokine production (41). This cytokine-suppressive binding protein was subsequently cloned and was identified as p38 MAPK (42).

While p38 MAPK plays a role in regulating inflammatory cytokine production as well as many other cellular responses to stress, the biological consequences of MAPK activation in the heart are diverse and not clearly understood. Recently, p38 MAPK has been implicated in cardiac hypertrophy, ischemia-reperfusion, and cardiomyocyte apoptosis (52, 55). Furthermore, Weinbrenner and colleagues (56) showed that upregulation of p38 MAPK activity correlates with ischemic preconditioning, most likely through the phosphorylation of heat shock protein 27 (40, 52). Some downstream targets of p38 MAPK activation may include several transcription factors including activating

Address for reprint requests and other correspondence: J. W. Horton, Dept. of Surgery, Univ. of Texas Southwestern Medical Center, 5323 Harry Hines Blvd., Dallas, TX 75390-9160 (E-mail: jureta.horton@UTSOUTHWESTERN.edu).

The costs of publication of this article were defrayed in part by the payment of page charges. The article must therefore be hereby marked "*advertisement*" in accordance with 18 U.S.C. Section 1734 solely to indicate this fact.

transcription factor 2 (ATF2), nuclear factor (NF)-κB, and p53 (43, 47, 51).

Because p38 MAPK activation appears to be involved in other cardiac abnormalities, it is possible that this MAPK may also mediate the contractile deficits observed in burn trauma. Therefore, the purpose of this present study was to determine whether burn trauma activates p38 MAPK in the heart; in addition, the effects of inhibiting cardiac MAPK activity on cardiomyocyte secretion of the inflammatory cytokine TNF-α and on cardiac mechanical function were studied.

MATERIALS AND METHODS

Experimental Animals

Adult Sprague-Dawley rats (Harlan Laboratories; Houston, TX) weighing 325–360 g were used throughout the study. Animals were allowed 5–6 days to acclimate to their surroundings. Commercial rat chow and tap water were available at will throughout the experimental protocol. All work described herein was approved by the University of Texas Southwestern Medical Center Institutional Animal Care and Research Advisory Committee and was performed according to the guidelines outlined in the "Guide for the Care and Use of Laboratory Animals" published by the American Physiological Society.

Catheter Placement and Burn Procedure

Rats were briefly anesthetized with methoxyflurane 18 h before the burn experiment. Body hair was closely clipped, the neck region was treated with a surgical scrub (Betadine), and a polyethylene (PE) catheter (PE-50 tubing) was inserted into the left carotid artery with the tip advanced to the level of the aortic arch. In addition, a PE catheter (PE-50) was placed in the right external jugular vein for administration of fluids. The catheters were filled with heparinized saline and exteriorized at the nape of the neck, and the skin was closed. After the animals had recovered from the anesthesia for catheter placement, they were housed in individual cages, and body temperature was maintained throughout the experimental period with a heating pad and a heating lamp.

Hemodynamic, metabolic, and hematological measurements were collected 18 h after catheter placement (preburn data); the animals were then deeply anesthetized with methoxyflurane and secured in a constructed template device as previously described (3, 25, 36). The surface area of the skin exposed through the template device was immersed in 100°C water for 12 s on each side; with the use of this technique, full-thickness dermal burns comprising 40% of the total body surface area were obtained. This burn technique produces complete destruction of the underlying neural tissue and a transient (<45 s) increase in internal body temperature of 1–3°C. Sham burn rats were subjected to an identical preparation except that they were immersed in room temperature water. After immersion, the rats were immediately dried, and each animal was placed in an individual cage; the external jugular catheter was then connected to a swivel device (model 923, Holter pump, Critikon; Tampa, FL) for fluid administration during the 24-h postburn period (4 $ml \cdot kg^{-1} \cdot$percent $burn^{-1}$ lactated Ringer solution, with one-half of the calculated volume given during the first 8-h postburn and the remaining volume given during the next 16-h postburn). In the control group, the external jugular vein was cannulated but no fluid resuscitation was administered. Twenty-four hours after burn injury (or sham burn), hemodynamic parameters including systemic blood pressure [using a model P23 ID, Gould-Statham pressure transducer (Gould; Oxnard, CA) connected to a model 7D Polygraph recorder (Grass Instruments; Quincy, MA)] and heart rate (using a model 7P4F tachycardiograph, Grass Instruments) were measured. A small sample of arterial blood (0.25 ml) was withdrawn from the arterial catheter for measuring packed cell volume, hematocrit, arterial pH, and blood gases. Body temperature was measured with a rectal temperature probe (model 44TA, YS1-Tele Thermometer, Yellow Springs Instruments; Yellow Springs, OH), and respiratory rate was monitored by counting respiratory movement.

Experimental Groups

All rats had catheters placed before inclusion in an experimental group. Eighteen hours after catheter placement, rats were randomly divided into two major experimental groups as follows: cutaneous burn injury over 40% of the total body surface area (n = 68) or sham burn injury (n = 66). These two experimental groups were then subdivided such that one-half of the sham burns (n = 33) and one-half of the burns (n = 34) were given the selective inhibitor of p38 MAPK SB203580 [4-(4-fluorophenyl)-2-(4-methyl-sulfinylphenyl)-5-(4-pyridinyl)imidazole, SmithKline Beecham Pharmaceuticals; Brocham Park, UK]. SB203580 was dissolved in 0.03 N HCl-0.5% tragacanth (Sigma; St. Louis, MO) and was administered by oral gavage at 6 mg/kg at 15 min and 6 and 22 h after either burn or sham burn (4, 6). The remaining sham (n = 33) and burn rats (n = 34) were given vehicle (0.03 N HCl-0.5% tragacanth) to serve as appropriate control groups. Initial studies were designed to measure the time course of p38 MAPK activation after burn trauma. For these studies, three hearts were collected from each of the four experimental groups at several time points after injury (30 min and 1, 2, 4, 6, 12, and 24 h). The hearts were cleared of fat and epicardial vessels, freeze-clamped in liquid nitrogen, and stored at −80°C until used for immunoprecipitation of p38 MAPK for in vitro kinase assay or Western blot analysis. Thirty-two rats were used to assess ventricular function 24 h after burn trauma (Langendorff perfusion); rats (n = 8 rats/group) from each of the four experimental groups (sham plus vehicle, sham plus inhibitor, burn plus vehicle, and burn plus inhibitor) were studied. Four to five rats from each of the four experimental groups were used to prepare cardiomyocytes 24 h after burn injury to assess TNF-α secretion by this cell population. The time frame selected to assess ventricular function and TNF-α secretion was based on previous studies (unpublished data) from our laboratory examining the time course of cardiac contractile defects, NF-κB activation, and myocyte secretion of inflammatory cytokines.

Isolated Perfused Hearts (Langendorff Model)

For studies of cardiac contraction and relaxation, awake animals were anticoagulated with heparin sodium (1000 units, Elkins-Sinn; Cherry Hill, NJ) 24-h postburn (or sham burn) and decapitated with a guillotine. The hearts were rapidly removed and placed in ice-cold (4°C) Krebs-Henseleit bicarbonate-buffered solution [containing (in mM) 118 NaCl, 4.7 KCl, 21 $NaHCO_3$, 2.5 $CaCl_2$, 1.2 $MgSO_4$, 1.2 KH_2PO_4, and 11 glucose]. All solutions were prepared on the day of experimental performance and bubbled with 95% O_2-5% CO_2 (pH 7.4; Po_2, 550 mmHg; Pco_2, 38 mmHg). A 17-gauge cannula placed in the ascending aorta was connected to a buffer-filled reservoir for perfusion of the coronary circulation at a constant flow rate of 5 ml/min. Hearts were suspended in a temperature-controlled chamber maintained at 38 ± 0.5°C,

and a constant flow pump (model 911, Holter pump, Critikom) was used to maintain perfusion of the coronary arteries by retrograde perfusion of the aortic stump cannula. Coronary perfusion pressure was measured and effluent was collected to confirm coronary flow rate. Contractile function was assessed by measuring intraventricular pressure with a saline-filled latex balloon placed in the left ventricular chamber. Left ventricular pressure (LVP) was measured with a Statham pressure transducer (model P23 ID, Gould) attached to the balloon cannula; the rate of LVP rise ($+dP/dt_{max}$) and fall ($-dP/dt_{max}$) was obtained using an electronic differentiator (model 7P20C, Grass Instruments) and recorded (model 7DWL8P, Grass Recording Instruments).

A Frank-Starling relationship for each heart was determined by plotting left ventricular developed pressure (peak systolic pressure minus left ventricular end-diastolic pressure) and $\pm dP/dt_{max}$ responses to increases in preload (left ventricular end-diastolic volume). Because the heart rate varied after burn injury, hearts were paced through an electrode attached to the right atrium (3–4 Hz, 2–10 W for 4-ms duration; Grass stimulator, Grass Instruments). Hearts were paced at twice the minimum capture voltage; thus in vitro heart rates were similar in all experimental groups, and differences in cardiac performance could not be attributed to burn-related differences in heart rate. In addition, ventricular performance was assessed in all hearts as coronary flow rate was increased from 3 to 12 ml/min or as perfusate calcium concentration was increased from 1 to 8 mM.

Cardiomyocyte Isolation

To isolate cardiac myocytes, animals from each experimental group were heparinized 24-h postburn and decapitated, and the hearts were removed through a medial sternotomy with the use of sterile techniques. The isolated heart was immediately placed in ice-cold calcium-free Tyrode solution [containing (in mM) 136 NaCl, 5 KCl, 0.57 $MgCl_2$, 0.33 NaH_2PO_4, 10 HEPES, and 10 glucose]. The aorta was cannulated within 60 s, and the excised heart was perfused with calcium-free Tyrode solution using a Langendorff perfusion apparatus. Perfusion was maintained for 5 min and then switched to a collagenase solution, which contained 80 ml of calcium-free Tyrode, 40 mg of collagenase A (0.05%, Boehringer Mannheim; Indianapolis, IN), and 4 mg of protease (Polysaccharide XIV, Sigma) with continuous oxygenation (95% O_2-5% CO_2). After this enzymatic digestion over a 10-min period was completed, the heart was removed from the cannula, and the ventricular tissue was separated from the base of the heart. This tissue was plated in a petri dish containing Tyrode solution with 100 μM calcium and gently minced to increase cell dispersion over 6 min. The myocyte suspension was then filtered, and the cells were allowed to settle. This rinsing and settling step was repeated three times with 10 min between each step and with gentle swirling between each step to allow myocyte separation. The calcium concentration of the rinsing solution was gradually increased during these steps from 100 to 200 μM and finally to 1.8 mM. The cell viability was measured (Trypan blue dye exclusion), and cell suspensions with >85% viability were used for subsequent studies. Myocytes with a rodlike shape, clearly defined edges, and sharp striations were prepared with a final cell count of 5×10^4 cells·ml^{-1}·well^{-1} (38).

Cytokine Secretion by Cardiomyocytes

Myocytes were pipetted into microtiter plates at 5×10^4 cells·ml^{-1}·well^{-1} (12-well cell culture cluster, Corning; Corning, NY) and subsequently stimulated with either 0, 10, 25, or 50 μg/well of LPS (from *Escherichia coli*; lot 65H 4053, Difco Laboratories; Detroit, MI) for 18 h (CO_2 incubator at 37°C). Supernatants were collected to measure myocyte-secreted TNF-α (TNF-α, rat ELISA, Endogen; Woburn, MA). We previously examined the contribution of contaminating cells (nonmyocytes) in our cardiomyocyte preparations using flow cytometry, cell staining (hematoxylin and eosin), and light microscopy. We confirmed that <2% of the total cell number in a myocyte preparation was noncardiomyocytes (33). Because our cardiomyocyte preparations were 98% pure, we concluded that the majority of the TNF-α measured in the cardiomyocyte supernatant was indeed cardiomyocyte derived.

In Vitro p38 MAPK Assay

The in vitro kinase assay was performed on rat heart tissue extracts in which p38 MAPK had been immunoprecipitated. Briefly, 100 μg of extract was incubated with 2 μg p38 antibody (courtesy of Dr. M. Cobb, Dept. of Pharmacology, Univ. of Texas Southwestern Medical Center, Dallas, TX; Santa Cruz Biotechnology; Santa Cruz, CA), lysis buffer [containing phosphate-buffered saline (pH 7.4), 1% Nonidet P-40, 0.5% sodium deoxycholate, 0.1% SDS, 0.1 mg/ml phenylmethylsulfonyl fluoride, 45 μg/μl aprotinin, 1 mM sodium orthovanadate, and 0.5 mM β-glycerophosphate], and protein A sepharose beads for 2 h at 4°C with gentle agitation. After sedimentation, the protein A sepharose beads were washed twice with lysis buffer, twice with buffer B [containing 0.25 M Tris (pH 7.6) and 0.1 M NaCl], and once with kinase buffer [containing 20 mM HEPES (pH 8.0) and 20 mM $MgCl_2$]. The resulting p38 MAPK immunoprecipitates were resuspended in 30 μl of kinase assay reaction buffer, which contained kinase buffer (as indicated above) plus 50 μM ATP, 15 μCi [γ-^{32}P]ATP, and 20 μg glutathione-*S*-transferase (GST)-ATF2 (Upstate Biotechnology; Lake Placid, NY). The kinase reaction was initiated by incubating the samples at 30°C for 30 min. Termination of the kinase reaction was accomplished by sedimentation of the beads and addition of the supernatant to Laemmli buffer. After the samples were boiled for 5 min, SDS-PAGE (12%) was used to separate the kinase reaction product, and autoradiography was then performed on the dried gel. A beta scintillation counter was used to quantify incorporation of radiolabel into the reaction product.

Western Blot Analysis

Protein samples (30 μg) were separated on a 12% SDS-polyacrylamide gel and transferred to a polyvinylidene difluoride membrane (Millipore; Bedford, MA). The membrane was blocked by a 1-h incubation in a Tris-buffered saline solution [containing 20 mM Tris (pH 7.6), 135 mM NaCl, and 0.1% Tween] containing 3% bovine serum albumin and 1% nonfat dry milk. The phospho-p38 antibody or phospho-c-Jun NH_2-terminal kinase (JNK) antibody (Santa Cruz Biotechnology) was then added to the membranes at a dilution of 1:400 and incubated for 1 h at room temperature. After the primary antibody incubation, the membrane was washed three times with Tris-buffered saline solution with 0.1% Tween. The secondary antibody was then added to the membrane (1:2,500, Promega; Madison, WI) and incubated for 1 h at room temperature. The membrane was again washed three times with Tris-buffered saline with 0.1% Tween. The bound antibodies were visualized by enhanced chemiluminescence (Amersham; Piscataway, NJ).

Table 1. *Hemodynamic and metabolic responses to burn trauma or to burn trauma with MAPK inhibitor*

	Vehicle-Treated Sham	Sham + p38 MAPK Inhibitor	Vehicle-Treated Burn	Burn + p38 MAPK Inhibitor
MAP, mmHg	126 ± 4	145 ± 3*	94 ± 4*	116 ± 6*†
HR, beats/min	480 ± 22	516 ± 12	433 ± 21*	513 ± 17†
Body temperature, °C	38.9 ± 0.3	38.9 ± 0.2	38.8 ± 0.2	38.7 ± 0.2
pH	7.45 ± 0.02	7.54 ± 0.02	7.48 ± 0.01	7.51 ± 0.02
Hct, %	37.4 ± 2.3	38.8 ± 0.6	28.3 ± 1.6*	31.6 ± 1.6*
PCV, %	39.5 ± 3.7	43.0 ± 1.4	35.5 ± 0.6*	35.0 ± 1.5*
P_{CO_2}, mmHg	29 ± 2	29 ± 2	26 ± 2*	25 ± 2*
P_{O_2}, mmHg	113 ± 5	117 ± 6	120 ± 5	110 ± 4

All values are means ± SE. MAP, mean arterial pressure; HR, heart rate; Hct, hematocrit; PCV, packed cell volume; MAPK, mitogen-activated protein kinase. *Significant difference among groups, $P < 0.05$. †Significant difference between burn groups, $P < 0.05$.

In Vitro Effects of MAPK Inhibitor

To examine the cell-specific effects of MAPK inhibition on cardiomyocyte secretion of TNF-α, myocytes were harvested from additional rats 24 h after either burn trauma ($n = 5$) or sham burn ($n = 5$). Myocytes (5×10^4 cells/well) were incubated (37°C) for 60 min in Tyrode solution containing 1.8 mM calcium. SB203580 (0.2 or 20 μM) was then added, and the myocytes were incubated for an additional 60 min. The supernatant was removed and replaced with fresh Tyrode solution containing 1.8 mM calcium. After viability measurements, cells were challenged with LPS (0, 10, 25, or 50 μg/well). After 18 h, supernatants were collected to measure myocyte secretion of TNF-α. In this manner, the cell-specific effects of the MAPK inhibitor on cytokine secretion by cardiac myocytes was assessed in vitro.

Statistical Analysis

All values are expressed as means ± SE. Analysis of variance (ANOVA) was used to assess an overall difference among the groups for each of the variables. Levene's test for equality of variance was used to suggest the multiple comparison procedure to be used if the ANOVA was significant. If equality of variance among the four groups was suggested, multiple comparison procedures were performed (Bonferroni). If inequality of variance was suggested, Tamhane's multiple comparisons were performed. P values <0.05 were considered statistically significant (analysis was performed using SPSS for Windows, version 7.5.1).

RESULTS

Effects of Burn Trauma

Survival and hemodynamic responses to burn injury. All animals survived the respective experimental protocols. Despite aggressive fluid resuscitation during the 24-h postburn period, mean arterial blood pressure (MABP) was significantly lower in rats with burns compared with that measured in the sham burn rats (Table 1). Packed cell volume and hematocrit fell significantly in all burn rats, and this hemodilution was attributed to the aggressive fluid resuscitation after burn trauma (Table 1).

Cardiac function after burn trauma. Cardiac contraction and relaxation deficits occurred in burns despite aggressive fluid resuscitation. As shown in Table 2, LVP, $\pm dP/dt_{max}$, left ventricular developed pressure at 40 mmHg, the time to peak tension, time to 90% relaxation of the ventricle, and the time to $-dP/dt_{max}$ were significantly lower in burn rats than values measured in sham burn rats. In addition, burn-mediated cardiac contractile deficits were evident from the left ventricular function curves. As seen in Fig. 1, Frank-Starling relationships calculated for burn rats were shifted downward and rightward compared with those calculated for vehicle-treated shams. In addition, burn

Table 2. *p38 MAPK inhibitor alters cardiodynamic responses to burn trauma*

	Vehicle-Treated Sham	Sham + p38 MAPK Inhibitor	Vehicle-Treated Burn	Burn + p38 MAPK Inhibitor
LVP, mmHg	88 ± 3	91 ± 3	65 ± 5*	80 ± 2†
$+dP/dt_{max}$, mmHg/s	2,192 ± 32	2,050 ± 71	1,321 ± 117*	2,067 ± 111†
$-dP/dt_{max}$, mmHg/s	1,776 ± 68	1,725 ± 25	999 ± 91*	1,625 ± 52†
$LVDP_{40}$, mmHg/s	1,987 ± 23	1,900 ± 71	1,249 ± 110*	1,845 ± 124†
TPP, ms	78.9 ± 1.1	84.0 ± 4.1	88.0 ± 3.9*	88.8 ± 3.0*
RT_{90}, ms	74.6 ± 2.0	82.5 ± 6.0	82.9 ± 2.0*	83.3 ± 2.7*
Time to $+dP/dt_{max}$, ms	45.9 ± 1.8	52.5 ± 2.0	49.1 ± 1.2	57.0 ± 2.4*†
Time to $-dP/dt_{max}$, ms	45.0 ± 1.6	46.2 ± 1.4	40.3 ± 0.5*	50.0 ± 0.2†
CPP, mmHg	49.2 ± 3.4	50.5 ± 3.3	52.9 ± 6.6	46.8 ± 6.6
CVR, mmHg/s	9.87 ± 0.67	10.1 ± 0.7	10.6 ± 1.32	9.35 ± 0.32
HR, beats/min	256 ± 18	266 ± 7	252 ± 13	258 ± 4

All values are means ± SE. LVP, left ventricular pressure; $+dP/dt_{max}$ and $-dP/dt_{max}$, rate of LVP rise and fall, respectively; $LVDP_{40}$, left ventricular developed pressure at 40 mmHg; TPP, time to peak pressure; RT_{90}, time to 90% relaxation; CPP, coronary perfusion pressure; CVR, coronary vascular resistance. *Significant difference among groups, $P < 0.05$ (ANOVA and Bonferroni). †Significant difference between burn groups, $P < 0.05$ (unpaired Student t-test).

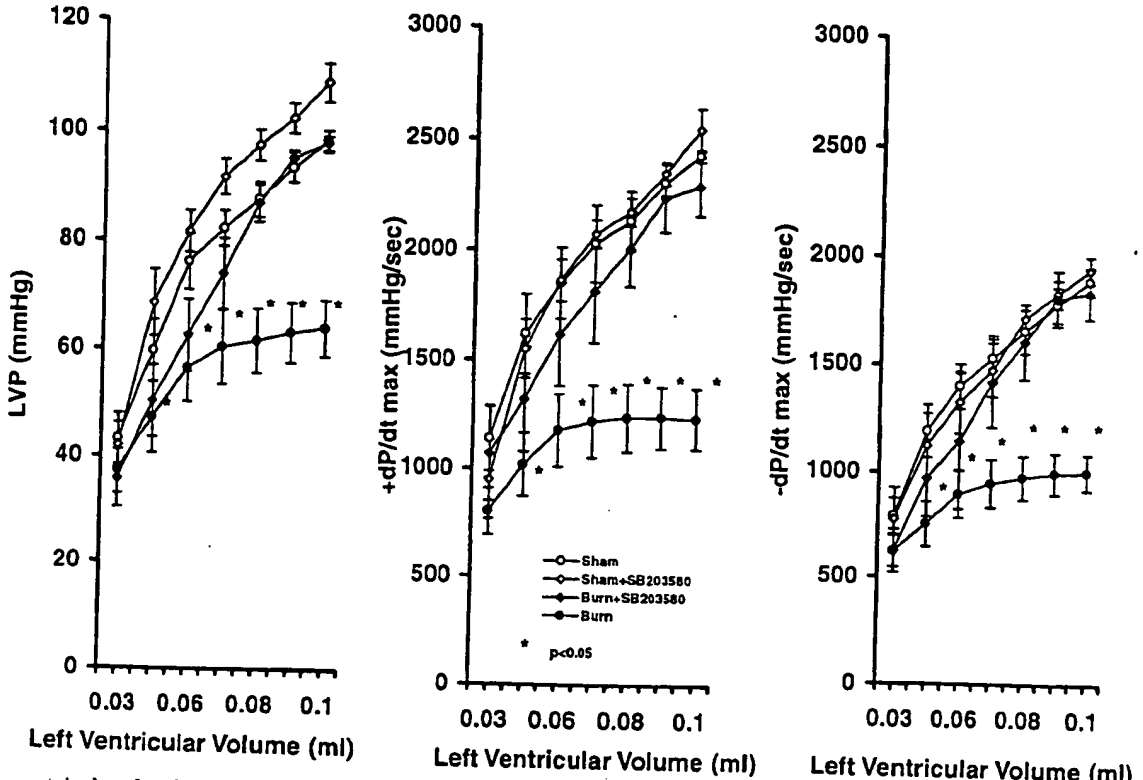

Fig. 1. Left ventricular developed pressure (LVP) calculated from peak systolic pressure minus end-diastolic pressure and the rate of LVP rise ($+dP/dt_{max}$) and fall ($-dP/dt_{max}$) responses to increases in preload (ventricular volume) (n = 8 animals/group). All values are means ± SE. Statistical analysis included ANOVA and a multiple comparison procedure (Bonferroni). *Significant difference among groups, $P < 0.05$.

trauma decreased ventricular responses to increases in coronary flow rate (Fig. 2) and to increases in perfusate calcium levels (Fig. 3).

p38 MAPK activity after burn trauma. To determine whether burn upregulated cardiac MAPK activity, hearts were collected at several time points after burn injury. As measured by Western blot, upregulation of p38 MAPK activity was observed as early as 1-h postburn (Fig. 4, *A* and *B*); this burn-mediated increase in p38 MAPK activity was confirmed by a specific p38 MAPK assay (Fig. 4*C*). Sixty minutes after burn trauma, p38 activity had increased from 1.28 ± 0.15 measured in the sham burn rats to 1.77 ± 0.055 relative units measured in the burn rats. Peak p38 MAPK activation occurred 2-h postburn, persisted through 4-h postburn, and returned to baseline values 6-h postburn (Fig. 4*C*).

Effects of MAPK Inhibition on Hemodynamic and Cardiodynamic Function

To determine whether upregulation of p38 MAPK plays a role in cardiac dysfunction after burn trauma, the specific p38 MAPK inhibitor SB203580 was administered with aggressive fluid resuscitation from burn trauma. A group of sham burn rats were treated with SB203580 to provide suitable controls. p38 MAPK inhibition in sham burn rats did not alter MABP, body temperature, or any measure of acid-base balance compared with those values measured in vehicle-treated sham rats (Table 1). While heart rate tended to increase after SB203580 administration in shams, this increase did not achieve statistical significance. Administration of the MAPK inhibitor in sham animals did not alter LVP, $\pm dP/dt_{max}$, time to peak tension, time to 90% relaxation, time to $\pm dP/dt_{max}$, coronary perfusion pressure, or coronary vascular resistance. Similarly, administration of the inhibitor in shams did not alter ventricular responsiveness to increases in left ventricular volume, increases in coronary flow rate, or increases in perfusate calcium concentration (Figs. 1–3).

MAPK inhibition in burn rats tended to improve MABP, but MABP remained significantly lower than values measured in the SB203580-treated sham rats. Inhibiting MAPK (by SB203580) in burn rats significantly improved LVP and $\pm dP/dt_{max}$, whereas burn-mediated changes in time to peak pressure, time to 90% relaxation of the ventricle, and time to $+dP/dt_{max}$ persisted. In addition, administration of SB203580 in burns significantly improved LVP and $\pm dP/dt_{max}$ responses to increases in ventricular volume (Fig. 1) and improved ventricular responsiveness to increases in either coronary flow rate (Fig. 2) or to increases in perfusate calcium (Fig. 3).

Effects of MAPK Inhibition on Cardiac MAPK/JNK Activity after Burn Trauma

To ensure that SB203580 blocked the MAPK pathway in the heart, p38 MAPK activity was determined

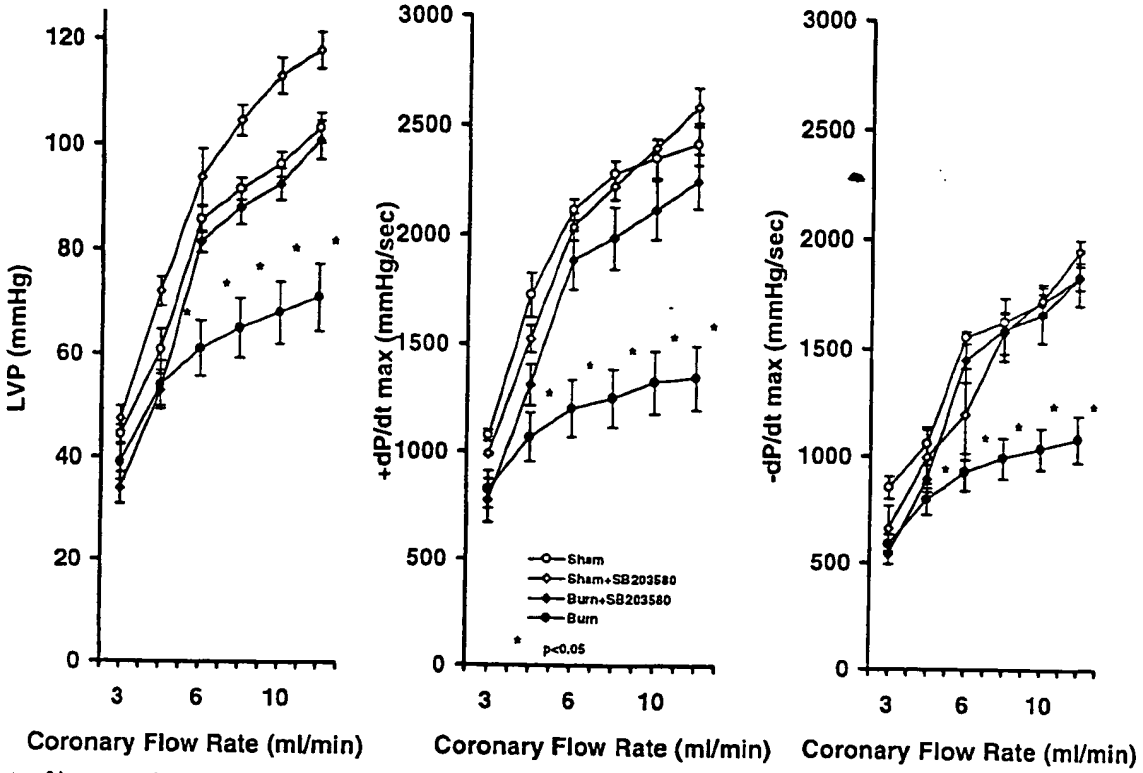

Fig. 2. Effects of increases in coronary flow rate on LVP and $\pm dP/dt_{max}$ in all experimental groups. All values are means ± SE. Statistical analysis included ANOVA and a multiple comparison procedure (Bonferroni). *Significant difference among groups, $P < 0.05$.

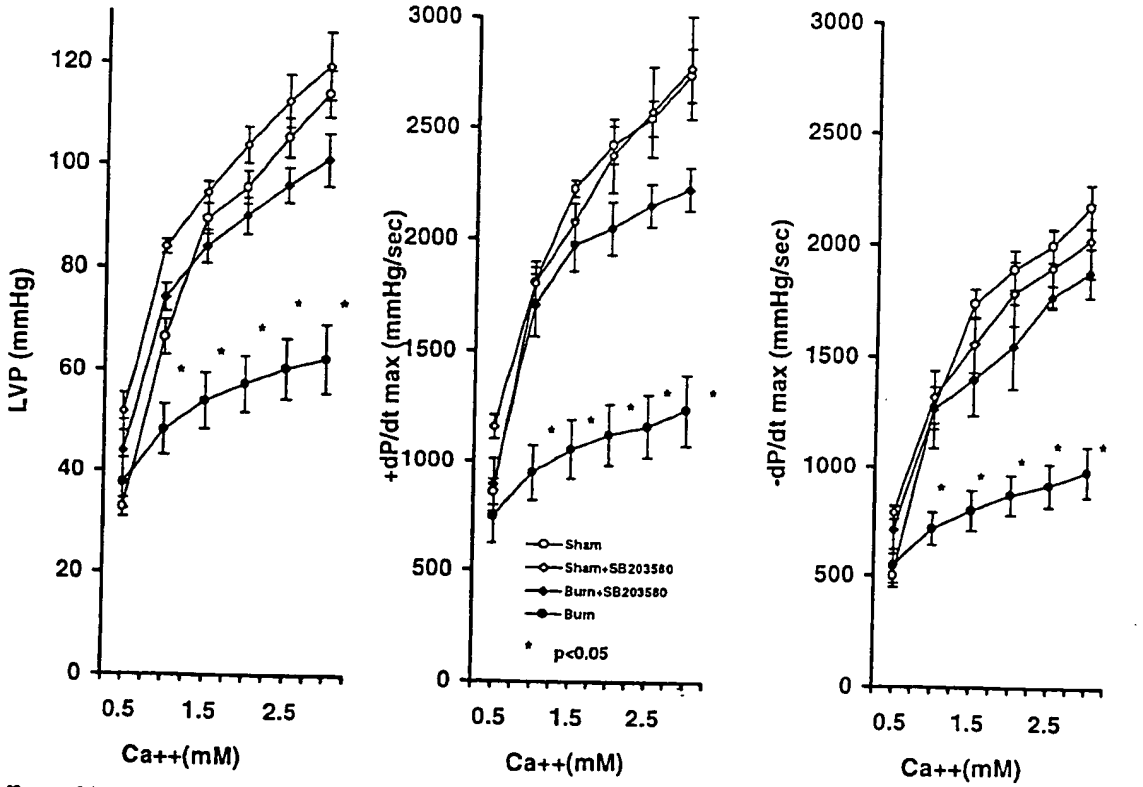

Fig. 3. The effects of increases in perfusate calcium levels on left ventricular contraction and relaxation in all experimental groups. All values are means ± SE. Statistical analysis included ANOVA and a multiple comparison procedure (Bonferroni). *Significant difference among groups, $P < 0.05$.

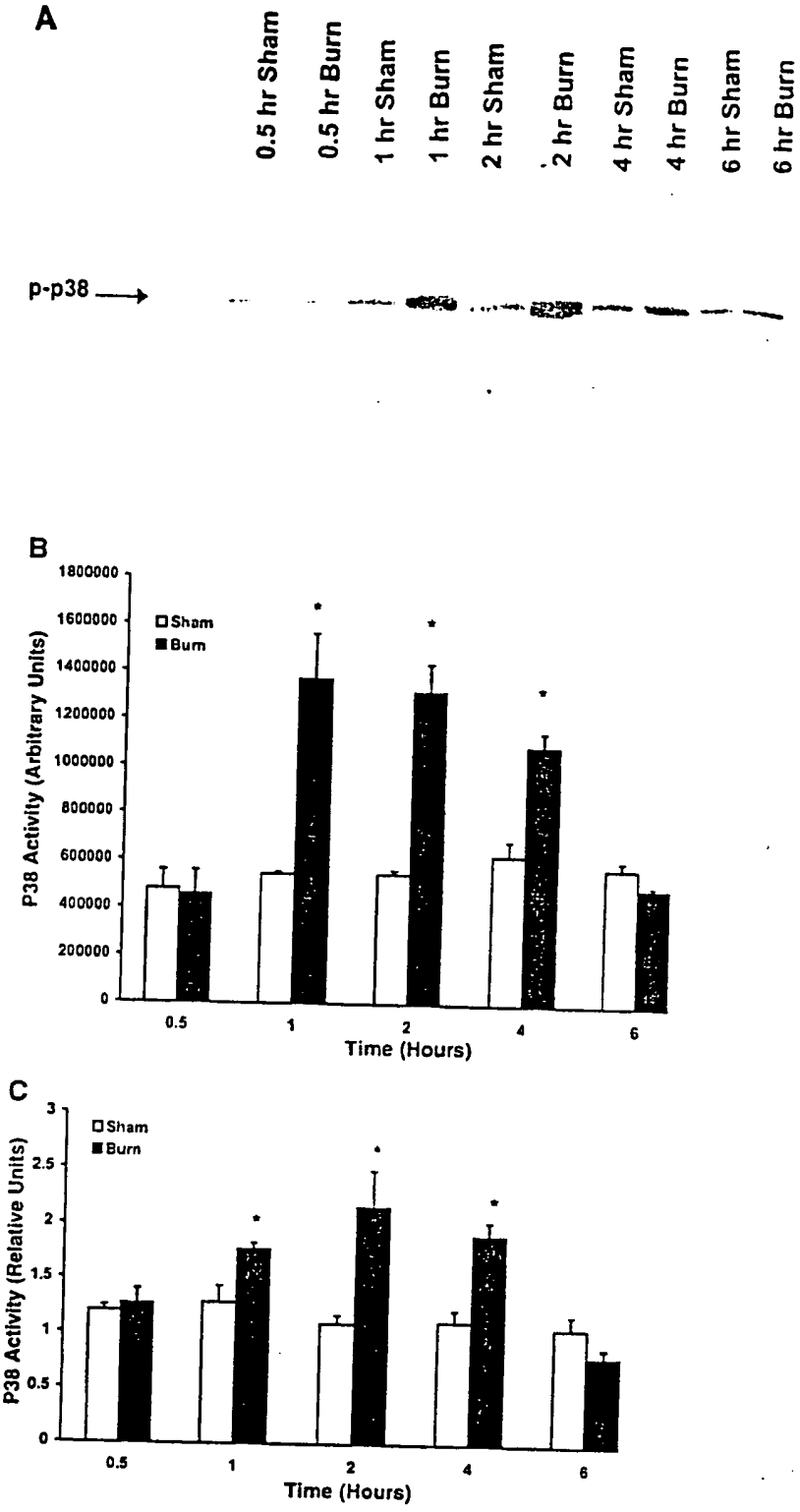

Fig. 4. Burn trauma activates p38 mitogen-activated protein kinase (MAPK) in the heart. *A*: Western blot analysis using an antibody that recognizes only the active, phosphorylated form of p38 MAPK (p-p38) indicated that upregulation of p38 MAPK activity occurred at 1-, 2-, and 4-h postburn. *B*: densitometric analysis of pooled anti-active p38 MAPK Western blots. *Significant increase in p38 MAPK activity (as indicated by p38 activity) in burn versus time-matched sham rats at 1-, 2-, and 4-h postburn, $P < 0.05$. *C*: in vitro p38 MAPK assay confirmed that burn trauma promoted activation of p38 MAPK (indicated as p38 activity) at 1-, 2-, and 4-h postburn. *Significant difference between burn and sham rats, $P < 0.05$.

in cardiac tissue harvested from the SB203580-treated experimental groups (SB203580-treated shams and SB203580-treated burn rats). This inhibitor abolished p38 MAPK activation at all times after burn injury; there were minimal effects of SB203580 in time-matched sham burn animals (Fig. 5, *A* and *B*). These data determined by Western blot were confirmed by an in vitro p38 MAPK specific assay (Fig. 5*C*). In addition, there was no effect of SB203580 on burn-mediated activation of JNK (Fig. 5*A*). Whereas burn trauma increased JNK activity in cardiac tissue, SB203580 had no significant effect on the burn-mediated increase in JNK activity.

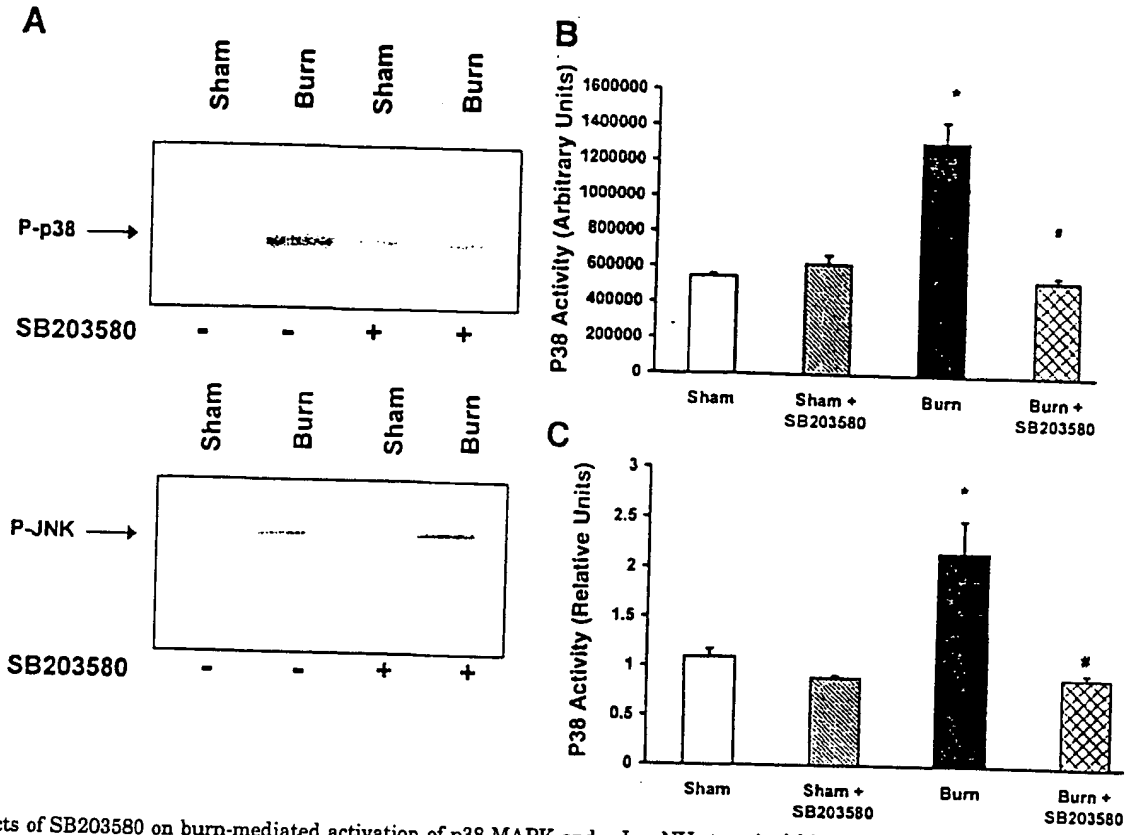

Fig. 5. Effects of SB203580 on burn-mediated activation of p38 MAPK and c-Jun NH_2-terminal kinase (JNK) in the heart. *A, top*: Western blot analysis with anti-active p38 MAPK antibody indicated that the burn-mediated increase in p38 MAPK activity (p-p38) at 2-h postburn was blocked by in vivo administration of SB203580. *Bottom*: Western blot analysis with anti-active JNK antibody demonstrated activation of JNK (p-JNK) 1-h postburn that was not inhibited by in vivo treatment with SB203580. + and −, Presence and absence, respectively, of SB203580. *B*: densitometric analysis of pooled anti-active p38 MAPK Western blots. *Significant elevation in p38 MAPK activity (indicated as p38 activity) in burn vs. sham rats, $P < 0.05$. #Significant difference in p38 MAPK activity in the SB203580-treated burn versus burn rats, $P < 0.05$. *C*: p38 MAPK assay confirmed that SB203580 prevented p38 MAPK activity (indicated as p38 activity) in burn rats. *Significant difference between burn and sham rats, $P < 0.05$. #Significant difference between vehicle-treated burn and SB203580-treated burn rats, $P < 0.05$.

Effects of MAPK Inhibition on Cardiac Myocyte Secretion of TNF-α

Primary cardiac myocytes were isolated from all four experimental groups (vehicle-treated sham, SB203580-treated sham, vehicle treated burn, and SB203580-treated burn rats). As shown in Fig. 6, burn trauma increased cardiac myocyte secretion of TNF-α ($P < 0.05$). Administration of the MAPK inhibitor during the postburn period significantly reduced this burn-mediated TNF-α response. Furthermore, MAPK inhibition during burn trauma produced cardiomyocyte TNF-α levels that were comparable to those measured in SB203580-treated sham burn rats.

As shown in Fig. 7, cardiomyocytes from vehicle-treated experimental groups responded to in vitro LPS challenge with a dose-dependent increase in TNF-α secretion ($P < 0.05$). However, cardiomyocytes harvested from vehicle-treated burn rats secreted significantly more TNF-α at each LPS concentration compared with the TNF-α responses measured in myocytes prepared from vehicle-treated sham rats ($P < 0.05$). Myocytes prepared from rats given SB203580 after burn trauma had reduced TNF-α responses to LPS challenge with significantly less TNF-α secreted at each LPS dose compared with those values measured in vehicle-treated burn rats ($P < 0.05$).

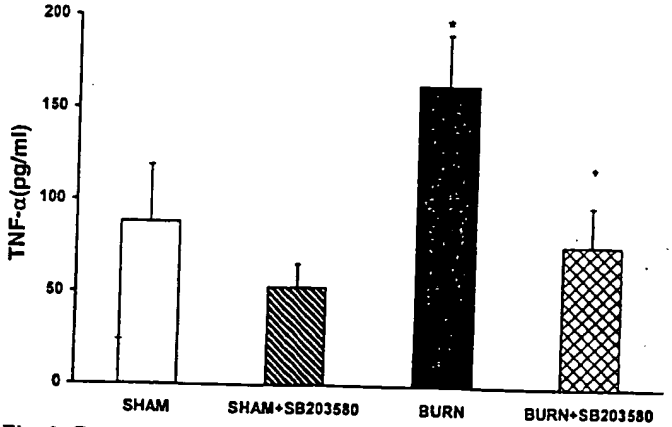

Fig. 6. Burn trauma produced a significant rise in cardiac myocyte secretion of tumor necrosis factor (TNF)-α at $P < 0.05$. All values are means ± SE. *Significant difference among groups, $P < 0.05$. †In vivo administration of the MAPK inhibitor SB203580 significantly reduced burn-mediated cytokine secretion by cardiac myocytes.

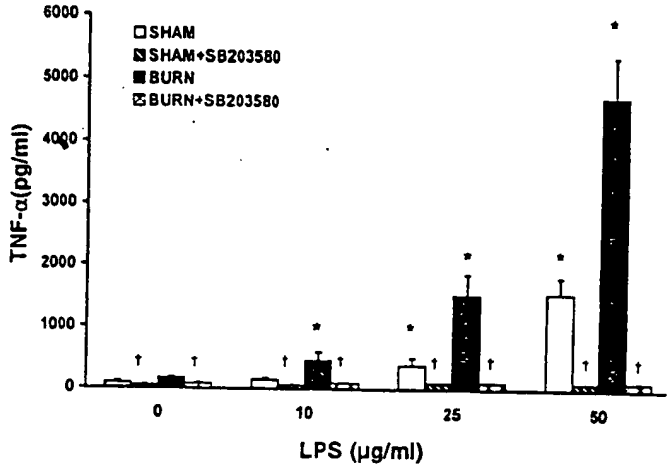

Fig. 7. Cardiac myocytes from vehicle-treated experimental groups responded to an in vitro lipopolysaccharide (LPS) challenge with a significant and dose-dependent increase in TNF-α secretion. All values are means ± SE. *Significant increase in cytokine secretion with LPS challenge compared with values measured in the respective experimental groups in the absence (0) of LPS. †Within each in vitro experimental challenge (i.e., at each LPS dose), in vivo administration of SB203580 reduced cardiomyocyte secretion of inflammatory cytokine by myocytes from both sham and burn rats (ANOVA and repeated measures).

In Vitro Effects of MAPK Inhibition on Cardiomyocyte Cytokine Secretion

Because the in vivo administration of the p38 MAPK inhibitor may affect cytokine production in both the reticuloendothelial system as well as by cardiac myocytes, the cell-specific effects of SB203580 on cardiac myocyte secretion of TNF-α were examined. This was accomplished by the in vitro addition of SB203580 to myocytes prepared from either sham burn or burn rats. The viability and morphological characteristics of myocytes harvested after exposure to either Tyrode solution alone or Tyrode solution containing SB203580 were nearly identical. As shown in Fig. 8, exposure of myocytes to SB203580 before LPS challenge significantly decreased myocyte secretion of TNF-α regardless of a previous burn injury. These data indicate the effects of p38 MAPK inhibition on TNF-α secretion were specific to the cardiac myocytes.

DISCUSSION

The data from this present study showed that burn trauma upregulated cardiac p38 MAPK activity, promoted secretion of the inflammatory cytokine TNF-α by cardiomyocytes, and impaired cardiac mechanical function. The in vivo administration of the selective p38 MAPK inhibitor SB203580 decreased burn-induced MAPK activity in the myocardium, abolished burn-mediated secretion of TNF-α by cardiac myocytes, and prevented postburn cardiac contractile dysfunction. In addition, in vitro treatment of cardiac myocytes with SB203580 inhibited the cytokine response elicited by LPS challenge.

We and others (34, 37, 48) confirmed that inflammatory cytokines such as TNF-α impair several aspects of cardiac contraction and relaxation. Further evidence that TNF-α produces cardiac contractile dysfunction has been provided by studies showing that 75-TNF receptor linked to the Fc portion of IgG-1 (an anti-TNF strategy) ablated systolic and diastolic cardiac dysfunction after experimental burn trauma or sepsis (24, 25) and in isolated hearts challenged with TNF-α (34). Because TNF-α mediates, at least in part, the cardiac mechanical defects that have been shown to occur after burn trauma, it was reasonable to expect that inhibiting one aspect of the signal transduction pathway that regulates TNF-α transcription and translation would provide a measure of postburn cardioprotection. Indeed, our finding that SB203580 inhibited cardiomyocyte secretion of TNF-α and prevented burn-mediated cardiac dysfunction is consistent with studies by Cain and colleagues (9), who reported that SB203580 diminished ischemia-induced TNF-α secretion and improved postischemic function in isolated atria trabeculae.

Because burn trauma elicits a systemic inflammatory cascade by stimulating cytokine synthesis in both cells of the reticuloendothelial system as well as in cardiac myocytes, the in vivo administration of SB203580 would likely interrupt several aspects of postburn inflammation. The question of whether this inhibitor would specifically target cardiac myocyte secretion of TNF-α was addressed by the in vitro studies where myocytes were pretreated with SB203580 before LPS challenge. The p38 MAPK inhibitor directly suppressed cytokine secretion elicited by LPS challenge of cardiac myocytes, suggesting that SB203580 can target cardiac myocytes.

Although little is known about the signaling pathway by which a cutaneous burn injury transmits an

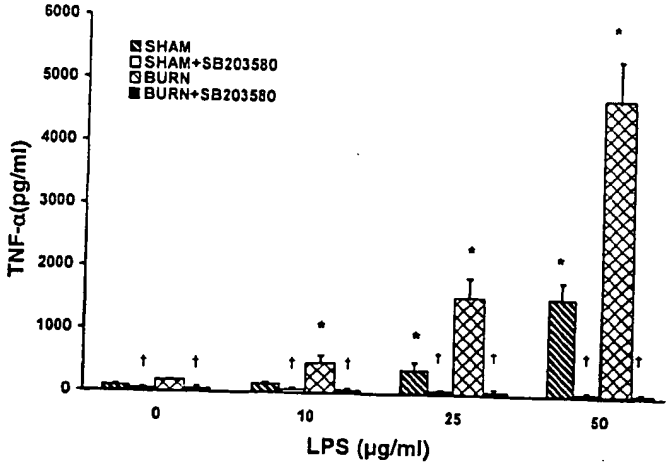

Fig. 8. These data describe the in vitro treatment (0.2 μM SB203580) of cardiac myocytes harvested after either sham or burn injury (24-h postburn). The addition of SB203580 to cardiac myocytes prepared from either sham or burn rats blunted the TNF secretory response to in vitro LPS challenge. All values are means ± SE. *Significant increase in cytokine secretion with LPS challenge compared with values measured in the respective experimental groups in the absence of LPS. †Within each in vitro experimental challenge (i.e., at each LPS dose), SB203580 reduced cardiomyocyte secretion of inflammatory cytokine by myocytes from both sham and burn rats (ANOVA and repeated measures).

extracellular stimulus to the nucleus to trigger an inflammatory response by cardiac myocytes, the data from this present study suggest that this pathway likely includes MAPK. Several previous studies (17, 18, 29, 30, 46, 54) proposed a significant role for LPS in this signaling cascade. It is well recognized that burn trauma promotes loss of gut mucosal barrier integrity and translocation of bacteria. While we failed to show a significant rise in serum LPS levels after burn trauma (unpublished data), the idea that LPS initiates a signal transduction pathway that culminates in cardiomyocyte TNF-α secretion has not been ruled out. In addition to LPS, it is clearly recognized that cutaneous burn promotes the formation of several reactive oxygen species (ROS) (31, 36), and several studies have suggested that ROS alter several aspects of inflammatory cytokine signaling. The in vivo administration of SB203580 in our study may have altered many of the upstream events, providing an indirect means of interrupting MAPK activation. There are no data, to our knowledge, regarding the effects of SB203580 on gut barrier function, LPS-LPS binding protein binding, or free radical generation. In this regard, Clerk and colleagues (12–14, 50) showed that ROS activate p38 MAPK pathway in cultured cardiac myocytes. Alternatively, emigration of activated leukocytes from the coronary microcirculation (35) or coronary endothelium-derived TNF-α (11) may serve as the initiating stimulus for postburn TNF-α secretion by cardiac myocytes. Because several putative burn-derived extracellular signals have been shown to activate p38 MAPK in other experimental models, our current finding that burn trauma upregulated the p38 MAPK pathway was not surprising.

Whereas the signal transduction cascade that regulates TNF-α synthesis and secretion by cardiac myocytes has not been defined in burn trauma, synthesis of inflammatory cytokines such as TNF-α by macrophages has been studied in considerable detail. In the macrophage population, LPS complexes with LPS binding protein and binds to CD14 (27, 57). Geppert et al. (23) have shown that the LPS-generated signal is then transmitted to regulate TNF-α transcription via the ras/raf-1/mitogen-activated protein or extracellular signal-regulated kinase (ERK) kinase (MEK)/ERK1,2 pathway (23). Similarly, Swantek et al. (53) showed that JNK activities are upregulated by macrophage exposure to LPS. In the present study, cardiomyocytes isolated from burn rats secreted significantly more TNF-α in response to LPS challenge than myocytes prepared from sham burn rats, and this effect was blocked by p38 MAPK inhibition with SB203580.

The MAPK inhibitor SB203580 is a pyridinyl imidiazole compound with potent inhibitory effects on cytokine production by LPS-stimulated human monocytes and thp-1 cells (a human monocytic cell line) (22, 42). In addition, the pyridinyl imidiazoles exhibit anti-inflammatory effects in several animal models (41) and have been shown to exert beneficial effects in experimental arthritis and in experimental endotoxin shock (4–6, 46). Although the specificity of SB203580 for p38 MAPK has been established by an absence of inhibitory effects of this compound on various other kinases (15), recently SB203580 was shown to inhibit JNK in rat neonatal ventricular myocytes. In these myocytes, the IC_{50} for p38 MAPK and JNK was 0.07 and 3–10 μM, respectively (14). Because 0.2 μM SB203580 was employed in this study, it was likely that this compound was specific for p38 MAPK at the dosage used. However, we chose to examine the effects of SB203580 on JNK activity in our model of burn trauma. Whereas burn injury produced significant JNK activation 1- and 2-h postburn, this activity was not inhibited by in vivo administration of SB203580, confirming the selectivity of this inhibitor for p38 MAPK.

While this present study confirms that burn trauma activates p38 MAPK in the myocardium, the downstream substrates for this kinase group within the heart remain undefined. One potential target in the p38 MAPK pathway is the redox-sensitive transcription factor NF-κB. Nuclear translocation of NF-κB has been shown to occur in the heart after burn trauma (32), and previous studies (43, 44) have confirmed that p38 MAPK activity promotes NF-κB activation in several tissues. Because NF-κB is one of the transcription factors involved in TNF-α gene transcription, it is likely that burn trauma and p38 MAPK upregulation promote the release of inflammatory cytokines via a NF-κB-dependent mechanism. In addition, AP1, a transcription factor that is also activated by p38 MAPK, may play a role in the transcriptional regulation of postburn inflammatory cytokine production. It must also be considered that the upregulation of the p38 MAPK pathway after burn trauma may induce inflammatory enzymes such as inducible nitric oxide synthase and cyclooxygenase-2 as well as the increased expression of adhesion proteins such as vascular cellular adhesion molecule-1 (5, 16, 26, 49).

While much of the previous work examining the activation and regulation of p38 MAPK pathway used noncardiac myocyte cells, this pathway is likely of primary importance in the myocardium under stressful conditions such as ischemia and reperfusion, trauma with blood loss, and burn trauma. The data from this present study clearly indicate that this kinase pathway is activated by burn trauma, and activation of this pathway occurs early in the postburn period (1 h) and occurs before other signaling events within the myocardium, such as nuclear translocation of NF-κB and cardiomyocyte secretion of TNF-α (32). Clear definition of the p38 MAPK pathway, including delineating upstream activators of this pathway as well as downstream targets, will likely provide potential sites for therapeutic intervention after major traumatic injury.

REFERENCES

1. **Abraham E, Glauser MP, Butler T, Barbino J, Gelmont D, Laterre PF, Kudsk K, Ha HAB, Otto C, Tobin E, Zwingelstein C, Lesslauer W, and Leighton A.** p55 Tumor necrosis factor receptor fusion protein in the treatment of patients with severe sepsis and septic shock. A randomized controlled multicenter trial. Ro 45-2081 Study Group. *JAMA* 277: 1531–1538, 1997.

2. **Abraham E, Wunderink R, Silverman H, Perl TM, Nasraway S, Levy H, Bone R, Wenzel RP, Balk R, Allred R, Pennington JE, and Wherry JC.** Efficacy and safety of monoclonal antibody to human tumor necrosis factor alpha in patients with sepsis syndrome. *JAMA* 273: 934–941, 1995.
3. **Adams HR, Baxter CR, and Izenberg SD.** Decreased contractility and compliance of the left ventricle as complications of thermal trauma. *Am Heart J* 108: 1477–1487, 1984.
4. **Badger AM, Bradbeer JN, Votta B, Lee JC, Adams JL, and Griswold DE.** Pharmacological profile of SB203580, a selective inhibitor of cytokine suppressive binding protein/p38 kinase, in animal models of arthritis, bone resorption, endotoxin shock and immune function. *J Pharmacol Exp Ther* 279: 1452–1461, 1996.
5. **Badger AM, Cook MN, Lark MW, Newman-Tarr TM, Swift BA, Nelson AH, Barone FC, and Kumar S.** SB 203580 inhibits p38 mitogen-activated protein kinase, nitric oxide production, and inducible nitric oxide synthase in bovine cartilage-derived chondrocytes. *J Immunol* 161: 467–473, 1998.
6. **Badger AM, Olivera D, Talmadge JE, and Hanna N.** Protective effect of SK&F 86002, a novel dual inhibitor of arachidonic acid metabolism, in murine models of endotoxin shock: Inhibition of tumor necrosis factor as a possible mechanism of action. *Circ Shock* 27: 51–61, 1989.
7. **Bryant D, Becker L, Richardson J, Shelton J, Franco F, Peshock R, Thompson M, and Giroir B.** Cardiac failure in transgenic mice with myocardial expression of tumor necrosis factor-alpha. *Circulation* 97: 1375–1381, 1998.
8. **Cain BS, Harken AH, and Meldrum DR.** Therapeutic strategies to reduce TNF-α mediated cardiac contractile depression following ischemia and reperfusion. *J Mol Cell Cardiol* 31: 931–947, 1999.
9. **Cain BS, Meldrum DR, Dinarello CA, Meng X, Joo KS, Banergee A, and Harken AH.** Tumor necrosis factor-α and interleukin-1β synergistically depress human myocardial function. *Crit Care Med* 27: 1309–1318, 1999.
10. **Cain BS, Meldrum DR, Meng X, Dinarello CA, Shames BO, Banerjee A, and Harken AH.** p38 MAPK inhibition decreases TNF-α production and enhances postischemic human myocardial function. *J Surg Res* 83: 7–12, 1999.
11. **Chan EL, Haudek SB, and Murphy JT.** NF-κB regulation of TNF-α mRNA expression in endotoxin stressed human coronary endothelial cells. *National ACS Committee On Trauma Resident Paper Competition, Reno, Nevada.* March 9, 2000.
12. **Clerk A, Michael A, and Sugden PH.** Stimulation of multiple mitogen-activated protein kinase sub-families by oxidative stress and phosphorylation of the small heat shock protein, HSP25/27, in neonatal ventricular myocytes. *Biochem J* 333: 581–589, 1998.
13. **Clerk A and Sugden PH.** Mitogen-activated protein kinases are activated by oxidative stress and cytokines in neonatal rat ventricular myocytes (Abstract). *Biochem Soc Trans* 25: 566S, 1997.
14. **Clerk A and Sugden PH.** The p38 MAPK inhibitor, SB203580, inhibits cardiac stress-activated protein kinases/C-jun N-terminal kinases (SAPKs/JNKs). *FEBS Lett* 426: 93–96, 1998.
15. **Cuenda A, Royse J, Doza YN, Meier R, Cohen P, Gallagher TF, Young PR, and Lee JC.** SB203580 is a specific inhibitor of a MAP kinase homologue which is stimulated by cellular stresses and interleukin-1. *FEBS Lett* 364: 229–233, 1995.
16. **Davis RJ.** Transcriptional regulation by MAP kinases. *Mol Reprod Dev* 42: 459–467, 1995.
17. **Deitch EA and Bridges RM.** Effect of stress and trauma on bacterial translocation from the gut. *J Surg Res* 42: 536–542, 1987.
18. **Deitch EA, Winterton J, and Berg R.** Thermal injury promotes bacterial translocation from the gastrointestinal tract in mice with impaired T-cell-mediated immunity. *Arch Surg* 121: 97–101, 1986.
19. **Dinarello CA, Gelfand JA, and Wolff SM.** Anticytokine strategies in the treatment of the systemic inflammatory response syndrome. *JAMA* 269: 1829–1835, 1993.
20. **Evans TJ, Moyes D, Carpenter A, Martin R, Loetscher H, Lesslauer W, and Cohen J.** Protective effect of 55- but not 75-kDa soluble tumor necrosis factor receptor-immunoglobin G fusion proteins in an animal model of gram-negative sepsis. *J Exp Med* 180: 2173–2179, 1994.
21. **Fisher SCJ, Opal SM, Dhainaut JF, Stephens S, Zimmerman JL, Nightingale P, Harris SJ, Schein RMH, Panacep EA, Vincent JL, Foulke GE, Warren EL, Garrard C, Park G, Bodmer MW, Cohen J, Linden CV, Cross AS, and Sadoff JC.** Influence of an anti-tumor necrosis factor monoclonal antibody on cytokine levels in patients with sepsis. *Crit Care Med* 21: 318–327, 1993.
22. **Gallager TF, Fier-Thompson SM, Garigipati RS, Sorenson ME, Smietana JM, Lee D, Bender PE, Lee JC, Laydon JT, Griswold DE, Chabot-Fletcher MD, Breton JJ, and Adams JL.** 2,4,5-Triarylimidiazole inhibitors of IL-1 biosynthesis. *Bioorg Med Chem* 5: 1171–1176, 1995.
23. **Geppert TD, Whitehurst CE, Thompson P, and Beutler KBK.** Lipopolysaccharide signals activation of tumor necrosis factor biosynthesis through the Ras/Raf-1/MEK/MAPK pathway. *Mol Med* 1: 93–103, 1994.
24. **Giroir B, Arteaga G, White J, and Horton J.** Prevention of endotoxin-induced myocardial dysfunction with TNF blockade or IL-1 blockade (Abstract). *Crit Care Med* 24, *Suppl*: A144, 1996.
25. **Giroir BP, Horton JW, White DJ, McIntyre KL, and Lin CQ.** Inhibition of tumor necrosis factor prevents myocardial dysfunction during burn shock. *Am J Physiol Heart Circ Physiol* 267: H118–H124, 1994.
26. **Guan Z, Buckman SY, Pentland AP, Templeton DJ, and Morrison AR.** Induction of cyclooxygenase-2 by the activated MEKK1→SEK1/MKK4→p38 mitogen-activated protein kinase pathway. *J Biol Chem* 273: 12901–12908, 1998.
27. **Hailman E, Lichenstein HS, Worfel MM, Miller DS, Johnson Da Kelley M, Busse LA, Zakowski MM, and Wright SD.** Lipopolysaccharide (LPS)-binding protein accelerates the binding of LPS to CD14. *J Exp Med* 179: 269–277, 1994.
28. **Han J, Lee JD, Tobias PS, and Ulevitch RJ.** Endotoxin induces rapid tyrosine phosphorylation in 70Z/3 cells expressing CD14. *J Biol Chem* 268: 25009–25014, 1993.
29. **Herndon DN and Zeigler ST.** Bacterial translocation after thermal injury. *Crit Care Med* 21: 50–54, 1993.
30. **Horton JW.** Bacterial translocation after burn injury: the contribution of ischemia and permeability changes. *Shock* 4: 286–290, 1994.
31. **Horton JW.** Oxygen free radicals contribute to postburn cardiac cell membrane dysfunction. *J Surg Res* 61: 97–102, 1996.
32. **Horton J, Maass D, Haudek S, and Giroir B.** The role of NF-κB in cardiac TNF-α secretion after trauma (Abstract). *Proc Am Assoc Surg Trauma*, 1999.
33. **Horton JW, Maass D, White J, and Sanders B.** Nitric oxide modulation of TNF-α induced cardiac contractile dysfunction is concentration dependent. *Am J Physiol Heart Circ Physiol* 278: H1955–H1965, 2000.
34. **Horton JW, Maass D, White J, and Sanders B.** Hypertonic saline dextran suppresses burn-related cytokine secretion by cardiomyocytes. *Am J Physiol Heart Circ Physiol* 280: 1591–1601, 2001.
35. **Horton JW, Mileski WJ, White DJ, and Lipsky P.** Monoclonal antibody to intercellular adhesion molecule-1 reduces cardiac contractile dysfunction after burn injury in rabbits. *J Surg Res* 64: 49–56, 1996.
36. **Horton JW and White DJ.** Role of xanthine oxidase and leukocytes in postburn cardiac dysfunction. *J Am Coll Surg* 181: 129–137, 1995.
37. **Kappadia S, Lee J, Torre-Amione G, Birdsall HH, Ma TS, and Mann DL.** Tumor necrosis factor-α gene and protein expression in adult feline myocardium after endotoxin administration. *J Clin Invest* 96: 1042–1052, 1995.
38. **Keller RS, Parker JL, Adams HR, and Rubin LJ.** Contractile dysfunction and inositol phosphates in ventricular myocytes isolated from endotoxemic guinea pigs (Abstract). *Circ Shock* 37: 29, 1992.
39. **Kumar A, Thota V, Dee L, Olson J, Uretz E, and Parillo JE.** Tumor necrosis factor-alpha and interleukin 1-beta are responsible for the in vitro myocardial cell depression induced by human septic shock serum. *J Exp Med* 183: 949–958, 1996.

40. **Lavoie JN, Lambert H, Hickey E, Weber LA, and Landry J.** Modulation of cellular thermoresistance and actin filament stability accompanies phosphorylation-induced changes in the oligomeric structure of heat shock protein 27. *Mol Cell Biol* 15: 505–516, 1995.
41. **Lee JC, Badger AM, Griswold DE, Dunnington D, Truneh A, Votta B, White JR, Young PR, and Bender PE.** Bicyclic imidiazoles as a novel class of cytokine biosynthesis inhibitors. *Ann NY Acad Sci* 696: 149–170, 1993.
42. **Lee JC, Laydon JT, McDonnel PC, Gallagher TF, Kumar S, Green D, McNulty D, Blumenthal MJ, Heys JR, Landvatter SW, Strickler JE, McLaughlin MM, Siemens IR, Fisher SM, Livi GP, White JR, Adams JL, and Young PR.** A protein kinase involved in the regulation of inflammatory cytokine biosynthesis. *Nature* 372: 739–745, 1994.
43. **Maulik N, Sato M, Price BD, and Das DK.** An essential role of NF-κB in tyrosine kinase signaling of p38 MAP kinase regulation of myocardial adaptation to ischemia. *FEBS Lett* 429: 365–369, 1998.
44. **Meldrum DR.** Tumor necrosis factor in the heart. *Am J Physiol Regulatory Integrative Comp Physiol* 274: R577–R595, 1998.
45. **Meldrum DR, Shenkar R, Sheridan BC, Cain BS, Abraham E, and Harken AH.** Hemorrhage activates myocardial NF-κB and increases tumor necrosis factor in the heart. *J Mol Cell Cardiol* 29: 2849–2854, 1997.
46. **Olivera DL, Esser KM, Lee JC, Greig RG, and Badger AM.** Beneficial effects of SK&F 105809, a novel cytokine-suppressive agent, in murine models of endotoxin shock. *Circ Shock* 37: 301–306, 1992.
47. **Ono K and Han J.** The p38 signal transduction pathway: Activation and function. *Cell Signal* 12: 1–13, 2000.
48. **Oral H, Dorn GW, and Mann DL.** Sphingosine mediates the immediate negative inotropic effects of tumor necrosis factor-α in the adult mammalian cardiac myocyte. *J Biol Chem* 272: 4836–4842, 1997.
49. **Pietersma A, Tilly BC, Gaestel M, de Jong N, Lee JC, Koster JF, and Sluiter W.** p38 Mitogen activated protein kinase regulates endothelial VCAM-1 expression at the post-transcriptional level. *Biochem Biophys Res Commun* 230: 44–48, 1997.
50. **Seko Y, Takahashi N, Tobe K, Kadowaki T, and Yazaki Y.** Hypoxia and hypoxia/reoxygenation activate $p65^{PAK}$, p38 mitogen-activated protein kinase (MAPK), and stress-activated protein kinase (SAPK) in cultured rat cardiac myocytes. *Biochem Biophys Res Commun* 239: 840–844, 1997.
51. **She QB, Chen N, and Dong Z.** ERKs and p38 kinase phosphorylate p53 protein at serine 14 in response to UV radiation. *J Biol Chem* 275: 20444–20449, 2000.
52. **Sugden PH and Clerk A.** "Stress-responsive" mitogen-activated protein kinases (c-Jun N-terminal kinases and p38 mitogen-activated protein kinases) in the myocardium. *Circ Res* 83: 345–352, 1998.
53. **Swantek JL, Cobb MH, and Geppert TD.** Jun N-terminal kinase/stress-activated protein kinase (JNK/SAPK) is required for lipopolysaccharide stimulation of tumor necrosis factor alpha (TNF-α) translation: glycacorticoids inhibit TNF-α translation by blocking JNK/SAPK. *Mol Cell Biol* 17: 6274–6282, 1997.
54. **Tokyay R, Zeigler ST, Traver DL, Stothert JC Jr, Loick HM, Heggers JP, and Herndon DN.** Postburn gastrointestinal vasoconstriction increases bacterial and endotoxin translocation. *J Appl Physiol* 74: 1521–1527, 1993.
55. **Wang Y, Huang S, Sah VP, Ross J, Brown JH, Han J, and Chien KR.** Cardiac muscle cell hypertrophy and apoptosis induced by distinct members of the p38 mitogen-activated protein kinase family. *J Biol Chem* 273: 2161–2168, 1998.
56. **Weinbrenner C, Liu GS, Cohen MV, and Downey JM.** Phosphorylation of tyrosine 182 of p38 mitogen-activated protein kinase correlates with the protection of preconditioning in the rabbit heart. *J Mol Cell Cardiol* 29: 2383–2391, 1997.
57. **Wright SD, Ramos RA, Tobias PS, Ulevitch RJ, and Mathison JC.** CD14, a receptor for complexes of lipopolysaccharide (LPS) and LPS binding protein. *Science* 249: 1431–1433, 1990.
58. **Yokoyama T, Vaca L, Rossen RD, Durante W, Hazarika P, and Mann DL.** Cellular basis for the negative inotropic effects of tumor necrosis factor-α in the adult mammalian cardiac myocyte. *J Clin Invest* 92: 2303–2312, 1993.